

Ion Beam Storage with Electron Cooler and Digital Feedback Damping in HIMAC Synchrotron

Kota Torikai¹⁾, Shinji Shibuya²⁾, Takeshi Nakamura³⁾ and Koji Noda¹⁾

¹⁾National Institute of Radiological Sciences (NIRS) Inage Ward 4-9-1, Chiba City, Chiba Prefecture, 263-8111, Japan, kota@nirs.go.jp

²⁾Accelerator Engineering Company (AEC) Inage Ward 4-9-1, Chiba City, Chiba Prefecture, 263-8111, Japan

³⁾Japan Synchrotron Radiation Research Institute (JASRI) 1-1-1, Kouto, Sayo-cho, Sayo-gun, Hyogo 679-5198 Japan

Ion beam storage with electron cooler (EC) has a possibility of increasing ion beam intensity and enhancing beam quality, in order to expand attractive industrial and medical applications field of the synchrotron. It is experimentally observed that the circulation orbit of the storage beam become unstable when the spatial beam density exceeds a certain value during the beam stacking with electron cooling, especially in the vertical direction. Concept of feedback damping has proved to be effective for suppressing the beam oscillation. Digital feedback damping is recently installed at the main ring in NIRS. This paper reports the experimental result of the analog feedback damping, and design process of the digital feedback system.

I. ION BEAM STORAGE AND APPLICATION PLANS IN HIMAC

Heavy Ion Medical Accelerator in Chiba (HIMAC) has started cancer treatment by carbon beam since 1994. HIMAC can accelerate ion species from proton to xenon up to 800MeV/u. HIMAC consists of three ion sources, one RFQ (800keV/u), one Alvarez linac (6MV/u) and two equivalent synchrotron rings. HIMAC supplies the carbon beam in the daytime for the treatment, and it supplies various ion species with different energy of ion beam in the nighttime for physics and biological experiments. Schematic overview and machine parameters of the HIMAC is illustrated in Fig. 1, and TABLE I. The upper and the lower synchrotron can be operated independently.

The electron cooler (EC) has been installed in the lower ring (Ref. 1). The ion cooling experiments has started from 2000. Fig. 2 shows the electron cooler. 6MeV/u Ar¹⁸⁺ has been mainly selected for the cooling experiment. For the beam stacking experiments, 6 MeV/u ion beam is injected at 1.6-3.3 sec intervals. The longitudinal and transverse emittance of the injected beam shrinks due to the effect of electron cooling.

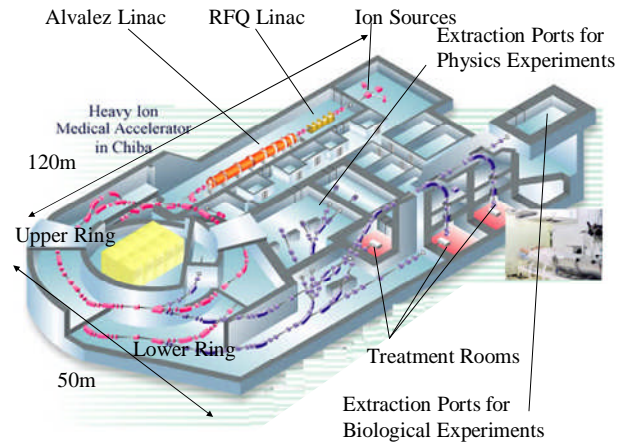


Fig. 1. Schematic overview of Heavy Ion Medical Accelerator in Chiba (HIMAC).

TABLE I. HIMAC Machine parameters

Circumference	129.6 m
Injection Energy	6 MeV/u
Lattice Type	FODO Lattice
Superperiod	6
Average Radius	20.6m
Tune(Q _x , Q _z)	(3.67-3.70, 3.13)
Transition Gamma	3.7
Acceptance(ϵ_x, ϵ_y)	(264, 26) π mm mrad
Repetition Time	3.3 sec
Vacuum	$\sim 10^{-8}$ Pa
Maximum Beam Energy	800MeV/u (Z/A=1/2)

Advantages of electron cooler on accelerator application are increase of the beam intensity and supply of small-emittance beam. One example of proposed applications for the former feature is a consecutive on-demand supply of the ion beam with response to an internal cancer position (Ref. 2, 3). Reduction of a

treatment time is directly linked to achieve more cost-conscious (Ref. 4) and more precise (Ref. 5) hadron therapy with satisfactory consistency. One example of proposed applications for the latter feature is a local irradiation by ion beams for tumor xenograft in model animal (Ref. 6). Production of small-size ion beam without collimation is earnestly required for estimating the irradiation dose precisely to elucidate the correlation with a clinical episode of effect / side effect to the threshold of allowable maximum dose.



Fig. 2. External view of the electron cooler at the lower synchrotron in HIMAC.

II. ELECTRON COOLING

TABLE III. Machine parameter of electron cooler

electron energy	3.4kV
cooling ion beam energy	6MeV/u
voltage stability	$\sim 10^{-4}$
electron current	80mA
solenoid length (cooling section)	1.0m
typical electron beam diameter	ϕ 100mm

II.A. Beam Stacking with Electron Cooling and Transverse Beam Instability

As well known, cool-stacking method can increase the beam intensity (Ref. 7). The maximum intensity through the cool-stacking is principally determined by a cooling time and a beam lifetime. As shown in Fig. 3, however, when the intensity exceeds 1.8mA the beam loss is suddenly occurred due to vertical coherent oscillation.

The maximum beam intensity during the beam stacking process is determined from the following condition: injection intervals, the ion density, cooling

strength, and magnitude of unstable beam oscillation. Fig. 3 represents the typical example of the beam stacking experiments with cooling.

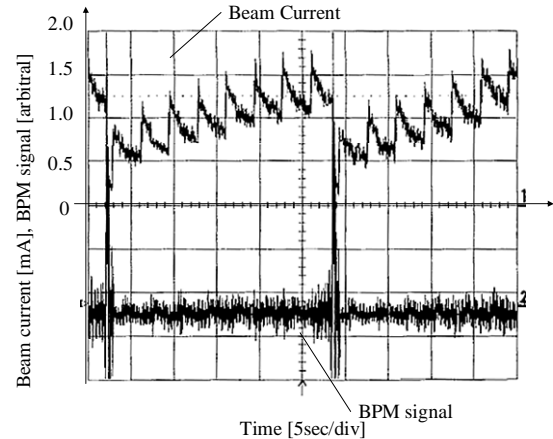


Fig. 3. Typical example of beam stacking experiments with electron cooling. Each of upper and lower waveform represents the time evolution of the beam intensity (0.5mA/div) and the output of the vertical beam position monitor (arbitrary unit).

II.B. Damping of Instability

Passive oscillation damping methods have been applied to the stacking experiment for suppressing the instability, especially in the vertical direction (Ref. 8). The first method is a changing of the working point from $(Q_x, Q_z) = (3.69, 3.13)$ to $(3.72, 2.89)$ in order to avoid approaching a coupling resonance condition of $Q_x - Q_z = 1$ or $Q_x + Q_z = 7$. The second method is an excitation of transverse RF for decreasing the ion density. The third method is a clearing of the secondary particles in the cooling section

Active feedback damping has been recently developed and applied in several accelerator facilities for stabilizing the transverse beam oscillation and ensure stable beam circulation (Ref. 9).

III. EXPERIMENT OF ANALOG FEEDBACK DAMPING

A feedback damping method has been applied for the cooling-stacking at the HIMAC synchrotron. The system is composed of the transverse beam position monitor, (BPM), amplifier, radio frequency-knockout (RF-KO) (Ref. 10) as transverse kicker and transmission line in

order to determine if the feedback is valid. Fig.4 and Fig.5 show the block diagram of transverse feedback damping system and picture of the RF-KO. A phase advance should be 90 deg between source signal from BPM and excitation signal of RF-KO. The phase advance can be adjusted by modulating the signal delay through the feedback system, under constant ion beam velocity.

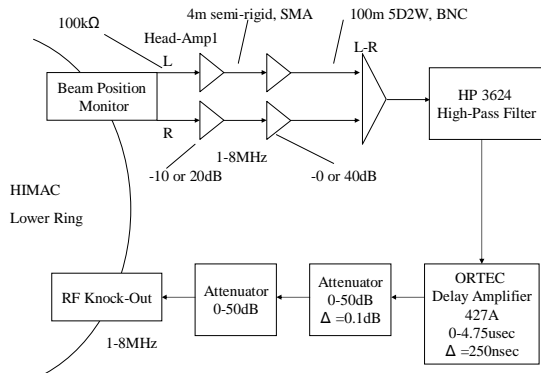


Fig. 4. Block diagram of the analog feedback damping system.

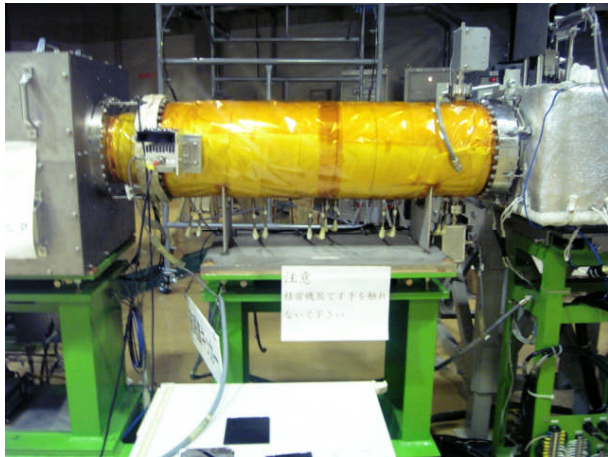


Fig. 5. Radio frequency-knockout (RF-KO) as an output electrode of feedback damping signal. Chamber length is 677mm. Size of embedded vertical electrode plates is width of 180mm, longitudinal length of 140mm and gap height of 50mm.

III.A. Observation of Feedback Damping with One Batch Injection

Analog feedback damping of single-injected beam with electron cooling was tested in prior to application to the cool-stacking. Measurement of a beam size during the cool-stacking seems difficult due to intermittent and

multiple beam injection. Fig. 6 represents the comparison of beam lifetime without / with feedback damping. Without feedback damping, unstable oscillation was occurred at 1.3sec after the injection. In contrast, with feedback damping, the oscillation was occurred at 2.3sec after the injection. This result indicates that analog feedback damping suppressed the vertical oscillations efficiently.

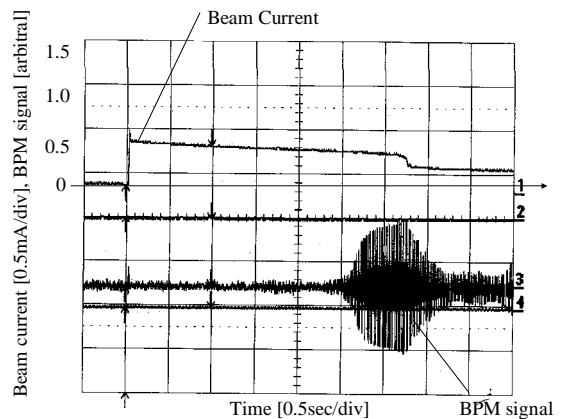
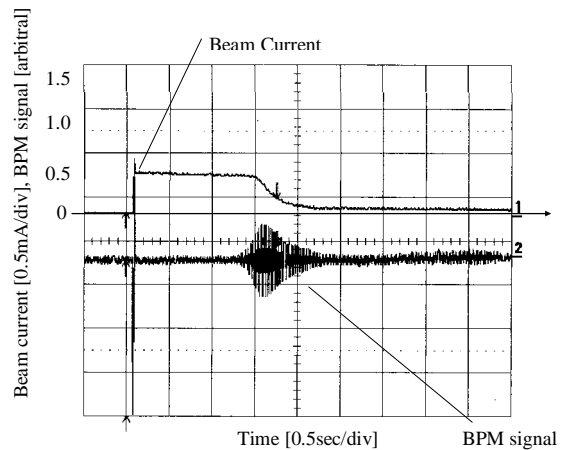


Fig. 6. Time evolution of beam current and vertical beam position without feedback damping (upper) and with feedback damping (lower).

III.B. Beam Stacking with Feedback Damping

The maximum stacked beam intensity and emergence of unstable oscillation is compared to evaluate the effect of feedback damping under cool-stacking. Fig. 7 represents the experimental result. Unstable oscillation

was observed without the damping, and the maximum beam intensity is limited to around 1.5mA. The vertical oscillation was effectively suppressed when the feedback damping is working. Change of beam lifetime due to the feedback damping is not observed.

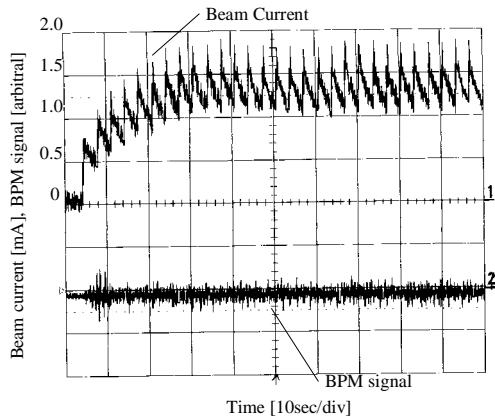
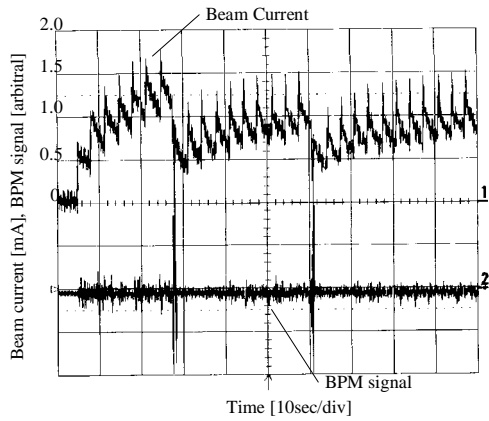


Fig. 7. Time evolution of beam intensity during the cool-stacking without feedback damping (upper) and with feedback damping (lower).

IV. SETUP OF DIGITAL FEEDBACK DAMPING SYSTEM

The digital feedback system (Ref. 9, 11) is categorized as a device of finite impulse response (FIR) filter. Fig. 8 represents a block diagram of the digital feedback system. The digital feedback system has advantageous features compared to the analog system. Adjust feasible cut-off frequency of the with appropriate phase-lag is simply done by changing coefficients of the FIR filter without modification of analog circuit. An internal delay by a buffer memory serves as the modulation of phase lag.

Input frequency of signal generator determines sampling frequency of the digital feedback system. The input frequency is set to an integral multiple of the revolution frequency. A required accuracy of the input frequency should be an order of 0.1% in order to avoid unnecessary aliasing noise.

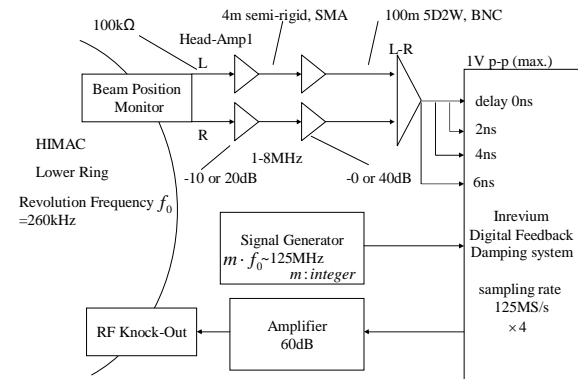


Fig. 8. Block diagram of the digital feedback damping system.

Fig. 9 shows an example of tune dependency of gain and phase delay implemented by the FIR filter. Design parameters of the gain and phase delay are the operating point, desired value of gain and phase of each tune fraction. In this example the frequency component of vertical betatron oscillation is transmitted to the output, and the component of horizontal betatron tune is slightly suppressed.

Fig. 10 shows an external view of the digital feedback system. The FPGA-based FIR filter is controlled via the Linux operating system. Number of 20 or 50 taps FIR filter can be chosen.

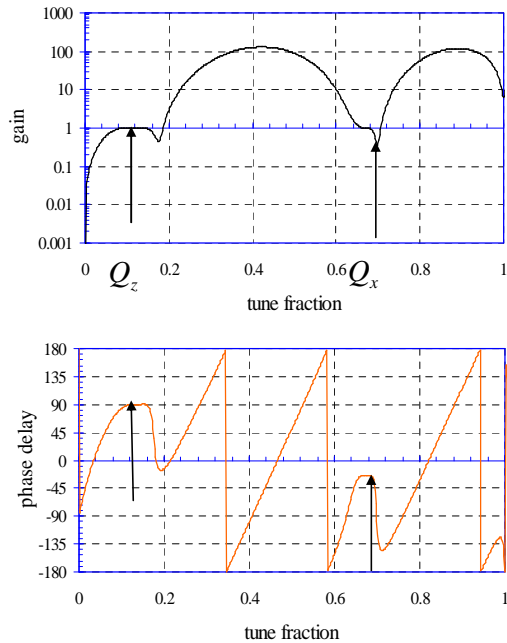


Fig. 9. Frequency dependence of designed FIR filter. Working point is $(Q_x, Q_z) = (3.69, 3.13)$.

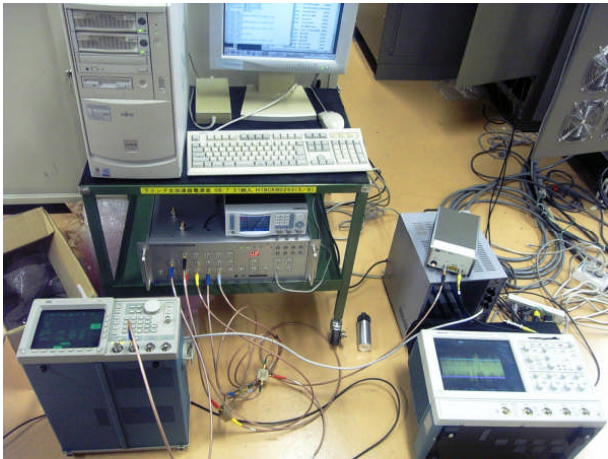


Fig.10 Experimental setup of the digital feedback damping.

V. SUMMARY

A concept of transverse feedback damping is tested in HIMAC. The analog feedback damping system efficiently suppresses the vertical oscillation during the beam stacking with electron cooling. The setup of digital feedback damping system is finished, and commissioning of the system is planned in this autumn. Optimization of the machine parameter for increasing beam lifetime and optimization of beam injection period, machine parameters and parameters of the electron cooler is required for obtaining higher beam intensity.

ACKNOWLEDGMENTS

The authors would express his sincere thanks to members of an accelerator group of NIRS for continuous encouragement and Accelerator Engineering Corporation for their skillful assistance in operating HIMAC accelerator complex. This work was carried out as a part of the Research Project with Heavy Ions at NIRS-HIMAC.

REFERENCES

1. K.NODA, T. MURAKAMI, E. TAKADA et al., *Nucl. Inst. Meth.* **A441**, pp. 159-166 (2000).
2. S. MINOHARA, T. KANAI, M. ENDO, K. NODA, and M. KANAZAWA, *Int J Radiat Oncol Biol Phys.* **47(4)**, pp. 1097-103 (2000).
3. H. SHIRATO, S. SHIMIZU, K. KITAMURA, and R. ONIMARU, *Int. J. Clin. Oncol.*, **12(1)**, pp. 8-16. (2007).
4. M. LODGE, M. PIJLS-JOHANNESM, L. STIRK et al., *Radiothr. Oncol.* **83(2)**, pp. 110-122 (2007).
5. T. FURUKAWA et al., *in this proceedings*.
6. S. TAKAHASHI, X. SUN, Y. KUBOTA et al., *J. Radiat. Res.*, **43**, pp. 143-152 (2002).
7. M. Grieser et al., *Proceedings of Tenth INS Symposium*, Japan, pp. 190-198 (1990).
8. T. UESUGI, K. NODA, E. SYRESIN et al., *Nucl. Inst. Meth.* **A545**, pp. 45-56 (2005).
9. T. NAKAMURA and K. KOBAYASHI, *Proceedings of ICALEPCS*, Geneva, 10-14 Oct. 2005, PO2.022-2, pp. 1-6 (2005).
10. K. NODA, T. FURUKAWA, S. SHIBUYA et al., *Nucl. Inst. Meth.* **A492**, pp. 241-252 (2002).
11. S. FUJIMOTO, T. SHIRAI, A. NODA et al., *Japanese Journal of Applied Physics*, **45**, 49, pp. L1307-L1310 (2006).